

## **A rapid and selective “on-off” fluorescence detection of lethal pulmonary agent phosgene supplemented with theoretical approach: a cost-effective sensing tool for household bleach and soil analysis**

Malavika S Kumar<sup>a</sup> Malay Dolai<sup>b</sup> and Avijit Kumar Das<sup>\*a</sup>

<sup>a</sup> Department of Chemistry, CHRIST (Deemed to be University), Hosur Road, Bangalore, Karnataka, 560029 India, Email: avijitkumar.das@christuniversity.in

<sup>b</sup> Department of Chemistry, Prabhat Kumar College, Contai, Purba Medinipur 721404, W.B., India.

### **CONTENTS**

<b>1. Preparation of phosgene gas .....</b>	<b>2</b>
<b>2. General methods of UV-vis and fluorescence titration experiments .....</b>	<b>2</b>
<b>3. Determination of fluorescence quantum yield.....</b>	<b>3</b>
<b>4. Calculation of the detection limit.....</b>	<b>3</b>
<b>5. Stern-Volmer plot and rate constant calculation.....</b>	<b>4</b>
<b>6. Job’s plot analysis and UV-vis spectra.....</b>	<b>5</b>
<b>7. NMR spectrum of DPBO .....</b>	<b>6</b>
<b>8. Mass spectra of DPBO and DPBO + COCl<sub>2</sub>.....</b>	<b>7</b>
<b>9. Plausible reaction mechanism .....</b>	<b>8</b>
<b>10. Soil analysis .....</b>	<b>8</b>
<b>11. Computational details.....</b>	<b>9</b>
<b>12. Comparison table.....</b>	<b>9-10</b>
<b>12. References.....</b>	<b>10</b>

## 1. Preparation of phosgene gas

As phosgene is toxic, volatile and difficult in handling hence, during the experiments we use less toxic, nonvolatile triphosgene ( $\text{CCl}_3\text{OC}(\text{O})\text{OCCL}_3$ ) as the precursor of phosgene gas. It generates phosgene gas in presence of triethylamine (TEA). In all the experiments acetonitrile has been used as solvent.

## 2. General method of UV-vis and fluorescence titration:

### By UV-vis method:

For UV-vis titrations, stock solution of the sensor was prepared ( $c = 2 \times 10^{-5}$  M) in  $\text{CH}_3\text{CN}$ . Triphosgene solution of concentration ( $c = 2 \times 10^{-4}$  M) was prepared in  $\text{CH}_3\text{CN}$  and Triethylamine was added to the solution (1:5 molar ratio). The solution of the guest interfering analytes like  $\text{CH}_3\text{COOH}$ ,  $\text{C}_4\text{H}_9\text{Cl}$ ,  $\text{C}_4\text{H}_9\text{Br}$ ,  $\text{C}_4\text{H}_9\text{I}$ ,  $\text{CH}_3\text{COCl}$ ,  $\text{C}_6\text{H}_5\text{COCl}$ ,  $\text{C}_6\text{H}_5\text{CH}_2\text{Cl}$ ,  $\text{SOCl}_2$  were also prepared in the order of ( $c = 2 \times 10^{-4}$  M). Initially sensor **DPBO** solution was prepared by dissolving the sensor in 2 ml acetonitrile followed by the gradual addition of corresponding guest analytes with the particular concentration. Solutions of various concentrations containing sensor and increasing concentrations of analytes were prepared separately. The spectra of these solutions were recorded by means of UV-vis methods.

### By fluorescence method:

For fluorescence titrations, stock solution of the sensor ( $c = 2 \times 10^{-5}$  M) was prepared for the titration of analytes in  $\text{CH}_3\text{CN}$ . Initially sensor **DPBO** solution was prepared by dissolving the sensor in 2 ml acetonitrile followed by the gradual addition of corresponding guest analytes with the particular concentration. The solution of the guest analytes in the order of  $2 \times 10^{-4}$  M were also prepared. Solutions of various concentrations containing sensor and increasing concentrations of analytes were prepared separately. The spectra of these solutions were recorded by means of fluorescence methods.

### General procedure for drawing Job's plot by UV-vis method:

A stock solution of the same concentration of **DPBO** and Phosgene was prepared in the order of  $\approx 2.0 \times 10^{-5}$  M in a  $\text{CH}_3\text{CN}$  ( $25^\circ\text{C}$ ) at pH 7.4. The absorbance in each case with different *host-guest* ratios but equal volumes (2 ml) was recorded. Job plots were drawn by plotting  $\Delta I$ .  $X_{\text{host}}$  vs  $X_{\text{host}}$  ( $\Delta I$  = change in the intensity of the absorbance spectrum during titration and  $X_{\text{host}}$  is the mole fraction of the host in each case, respectively).

### 3. Determination of fluorescence quantum yield:

Here, the quantum yield  $\phi$  was measured by using the following equation,

$$\phi_x = \phi_s (F_x / F_s)(A_s / A_x)(n_x^2 / n_s^2)$$

Where,

X & S indicate the unknown and standard solution respectively,  $\phi$  = quantum yield,

F = area under the emission curve, A = absorbance at the excitation wave length,

n = index of refraction of the solvent. Here  $\phi$  measurements were performed using anthracene in ethanol as standard [ $\phi = 0.27$ ] (error ~ 10%)

### 4. Calculation of the detection limit:

The detection limit DL of **DPBO** for phosgene was determined from the following equation:<sup>1</sup>

$$DL = K * Sb_1 / S$$

Where K = 2 or 3 (we take 3 in this case);  $Sb_1$  is the standard deviation of the blank solution; S is the slope of the calibration curve.

From the graph Fig.S1, we get slope = 0.8374, and  $Sb_1$  value is 6.0097.

Thus using the formula, we get the Detection Limit for phosgene = 21.53  $\mu$ M.

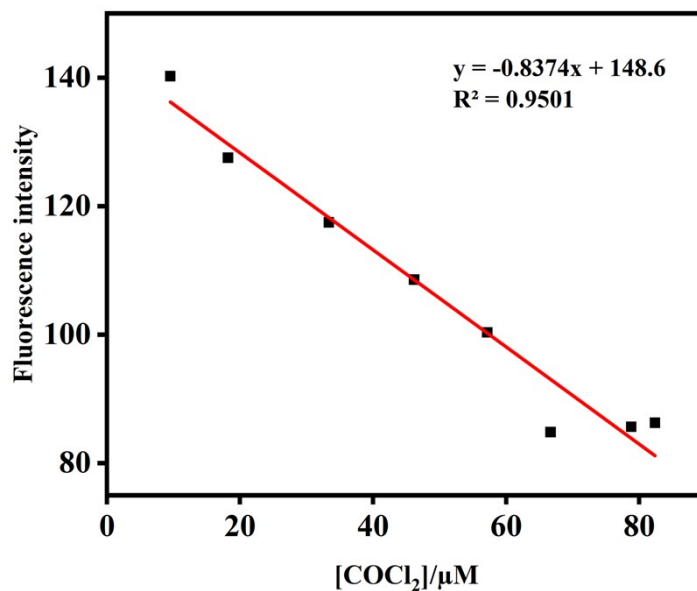


**Fig. S1:** Changes of fluorescence Intensity of **DPBO** as a function of [COCl<sub>2</sub>].

## 5. Stern–Volmer (SV) plot:

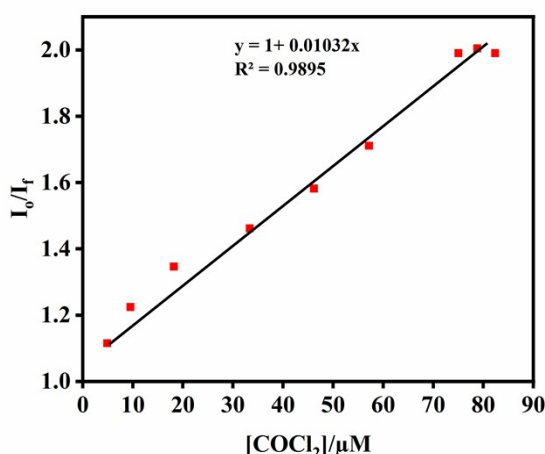


**Fig. S2:** Stern-Volmer plot of **DPBO** towards  $\text{COCl}_2$ .

The quenching efficiency and sensitivity were evaluated by calculating the Stern–Volmer quenching constant ( $K_{SV}$ ), calculated by the Stern–Volmer (SV) equation:  $I_0/I = 1 + K_{SV}[\text{COCl}_2]$ , where  $K_{SV}$  is the quenching constant ( $\text{M}^{-1}$ ),  $I_0$  and  $I$  are the fluorescence intensities of complexes before and after the addition of phosgene, and  $[\text{COCl}_2]$  is the molar concentration of phosgene.

## 6. The changes of emission curve of DPBO ( $c = 2 \times 10^{-5} \text{M}$ ) at different time interval by addition of phosgene ( $c = 2 \times 10^{-4}$ ) and calculation of first order rate constant:

Fig.S3 represents the changes of emission intensity at different time interval by addition of triphosgene/TEA. From the time vs. fluorescent intensity plot at fixed wavelength at 449 nm by using first order rate equation we get the rate constant  $K = \text{slope} \times 2.303 = 1.5659 \times 2.303 = 3.606 \text{ Sec}^{-1}$ .

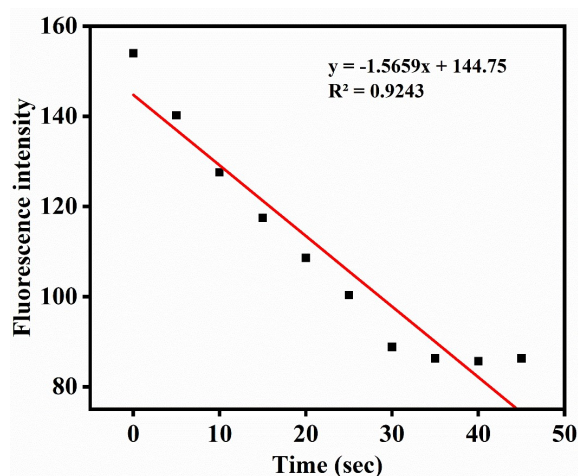


**Fig. S3.** The first order rate equation by using Time vs. fluorescence intensity plot at 449 nm.

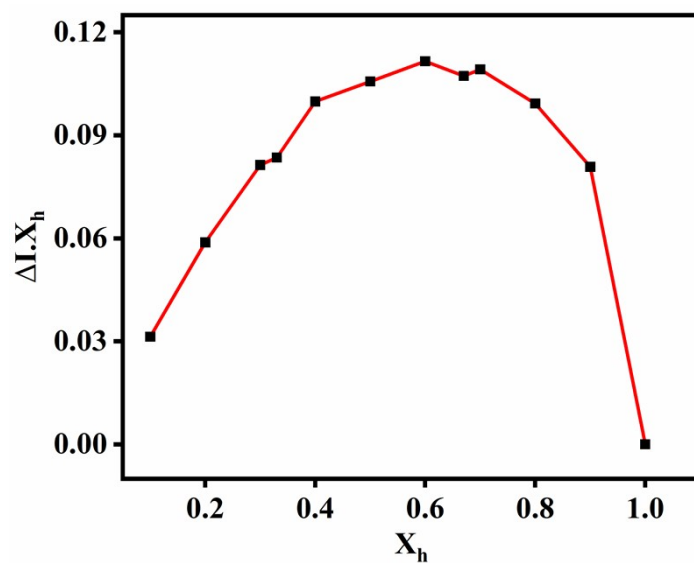


**Fig. S4.** Job plot diagram of **DPBO** with phosgene (where  $X_h$  is the mole fraction of the **DPBO** and  $\Delta I$  indicates the changes of the absorbance).

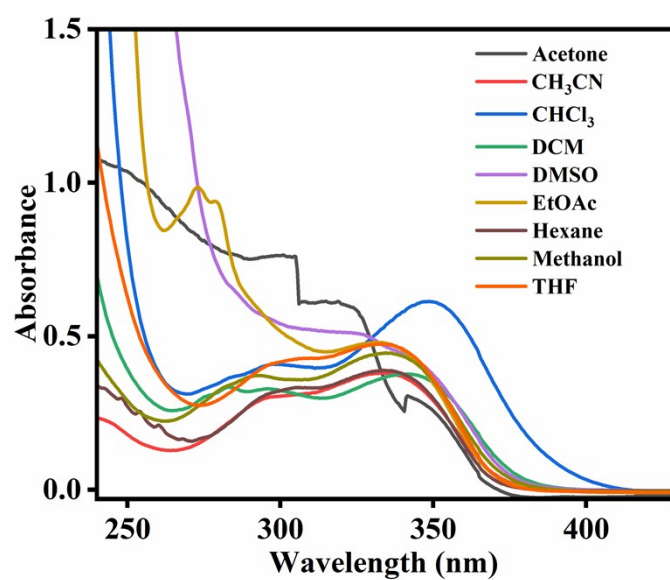


**Fig. S5.** UV-vis spectra of **DPBO** ( $c = 2.0 \times 10^{-5} \text{ M}$ ) in various solvents.

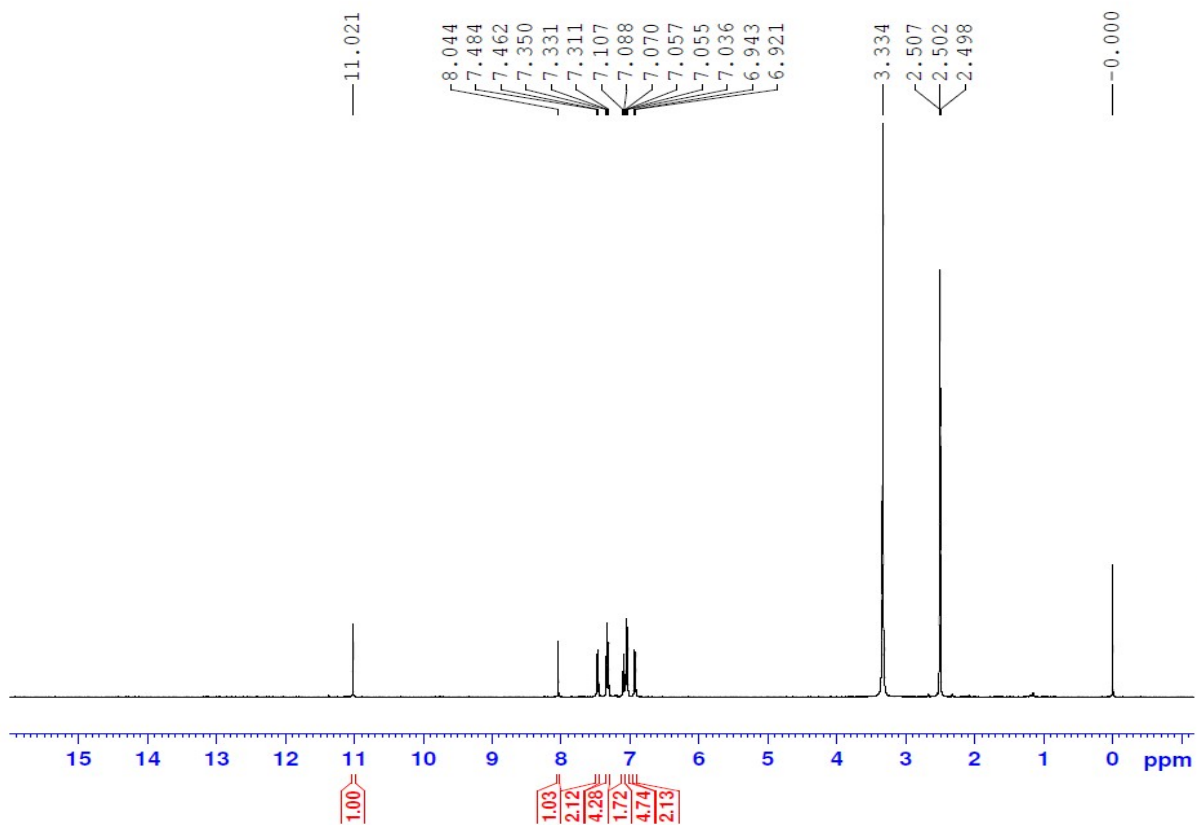


Fig.S6.  $^1\text{H}$  NMR spectrum of DPBO

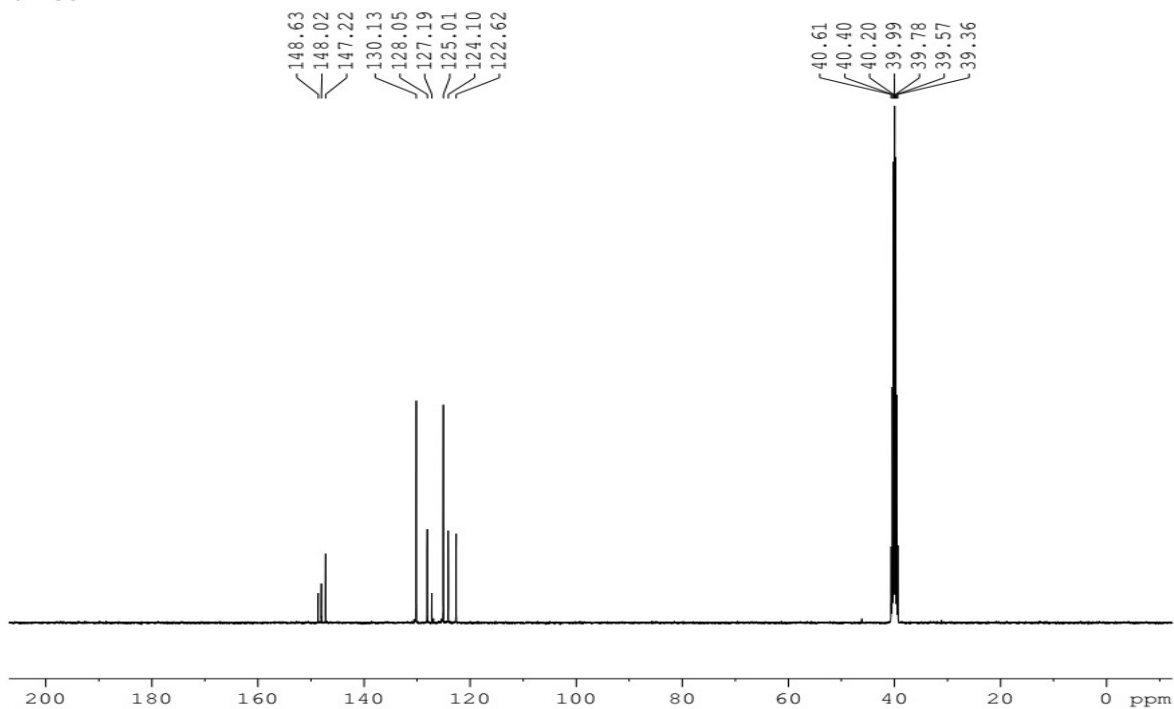
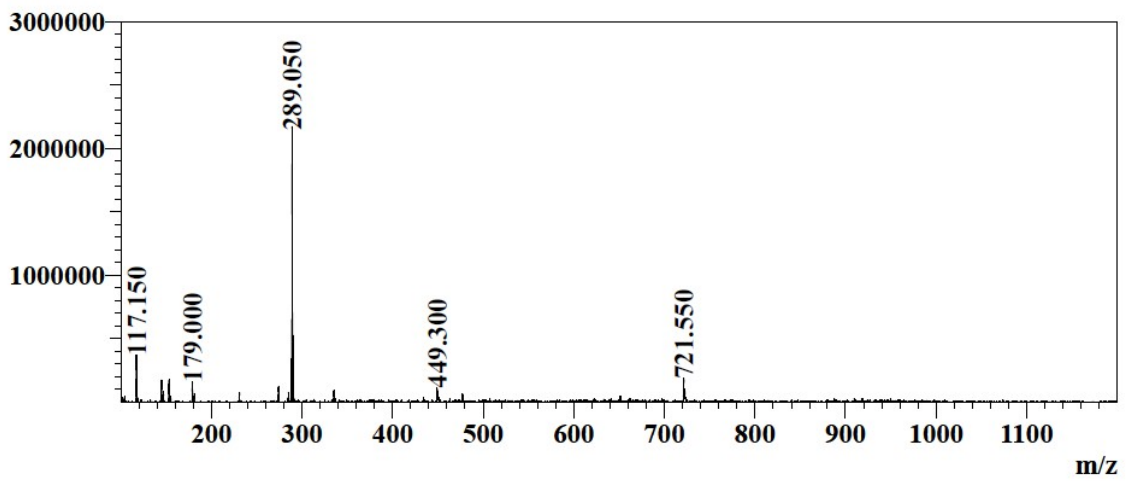
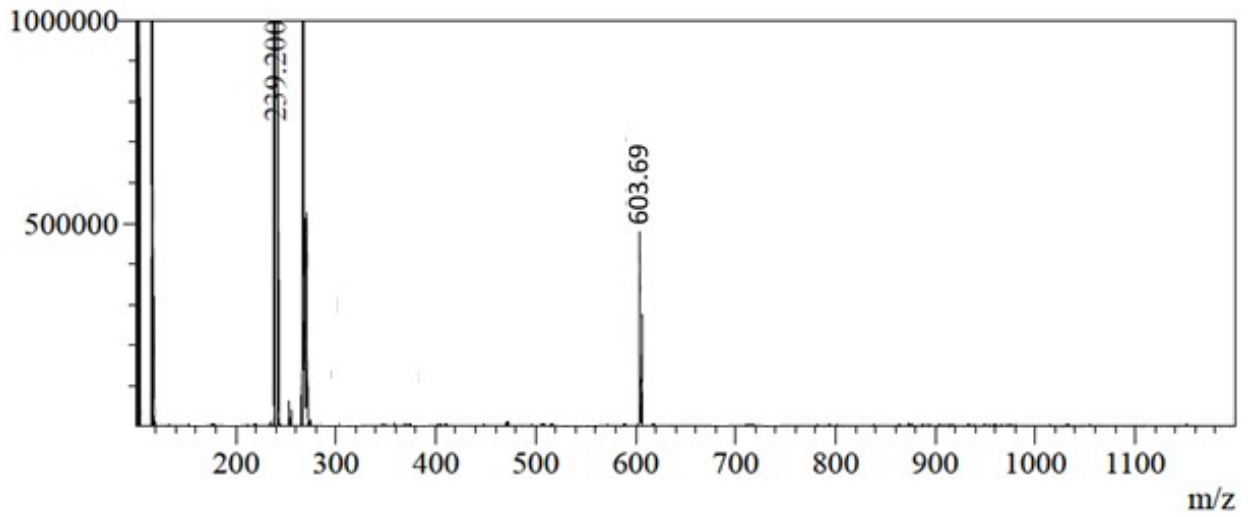


Fig.S7.  $^{13}\text{C}$ -NMR spectrum of DPBO



**Fig.S8. Mass spectrum of DPBO**



**Fig.S9. Mass spectrum of DPBO + phosgene**

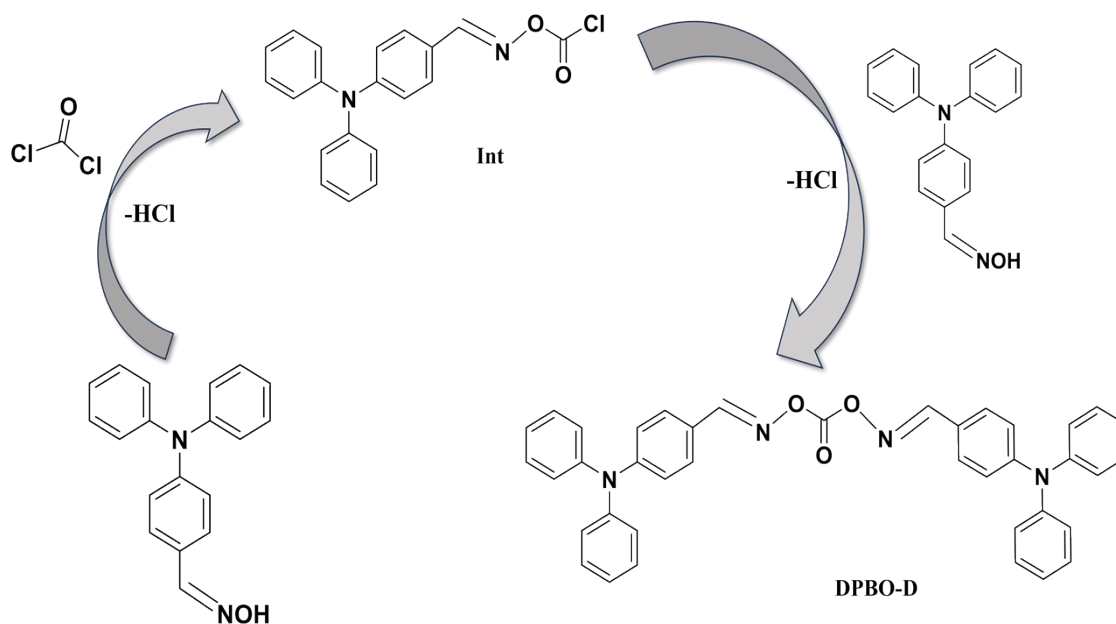


**Fig. S10** A plausible mechanism of interaction of **DPBO** with phosgene.

## 7. Soil Analysis

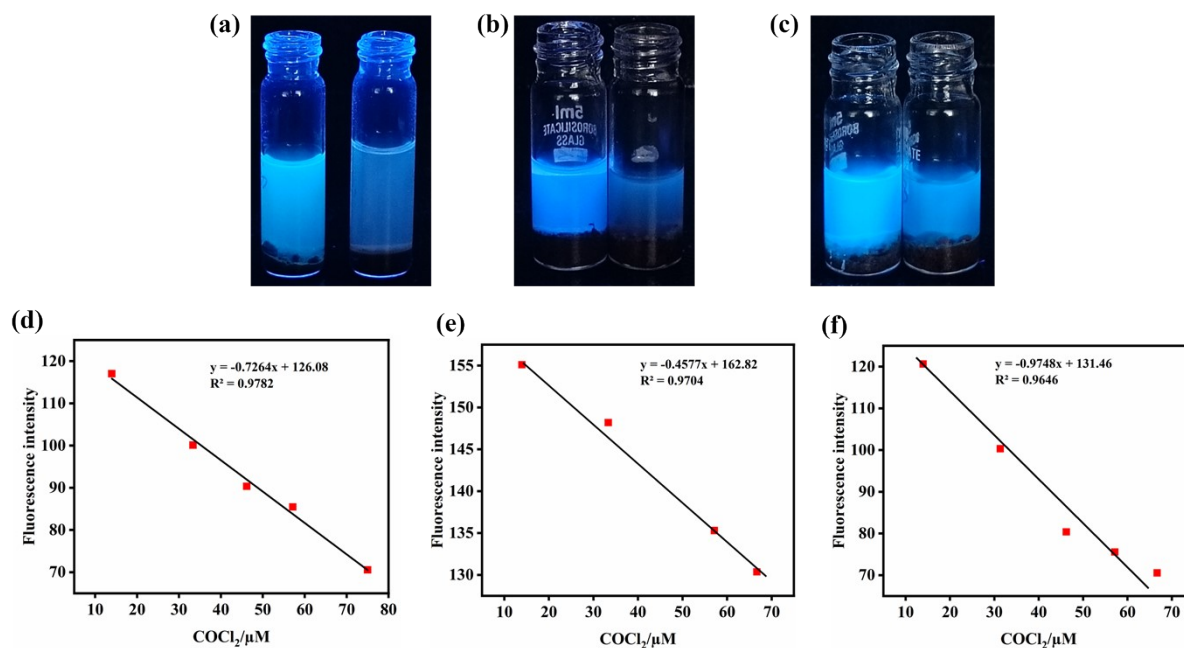


**Fig. S11** (a-c) Images of **DPBO** solution treated without (left) and with phosgene (right) for clay soil, Field soil and sandy soil respectively. (d-f) Emission changes of **DPBO** ( $c = 0.2 \mu\text{M}$ ) at 449 nm with different concentration of phosgene ( $c = 0.02 \mu\text{M}$ ).



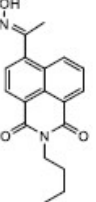
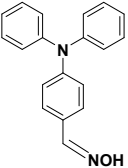
## 8. Computational details

Ground state electronic structure calculations for **DPBO** and phosgene bridged final product (**Bound**) in gas phase have been carried out using DFT<sup>2</sup> method associated with the conductor-like polarizable continuum model (CPCM).<sup>3</sup> Becke's hybrid function<sup>4</sup> with the Lee-Yang-Parr (LYP) correlation function<sup>5</sup> was used for the study. The absorbance spectral properties in MeCN medium for phosgene bridged product (**Bound**) were calculated by time-dependent density functional theory (TDDFT)<sup>6</sup> associated with the conductor-like polarizable continuum model and we computed the lowest 40 singlet – singlet transition.

For H, C, N, O, atoms we used 6-31+(g) basis set for all the calculations. The calculated electron-density plots for frontier molecular orbitals were prepared by using Gauss View 5.1 software. All the calculations were performed with the Gaussian 09W software package.<sup>7</sup>

## 9. Table S1: Comparison table of **DPBO** with the reported similar type of chemosensors

Ligands	Analytes	Solvent used	Probe type	Detection limit	Applications	References
	Phosgene	CH <sub>3</sub> CN	Turn off	1.52 nM	Detection of phosgene in household bleach	[8]
	Phosgene	CH <sub>3</sub> CN	Turn on	0.48 nM	Dipstick method	[9]
	Phosgene	1,4-dioxane solvent	Turn on	22.83 nM	Soil analysis	[10]
	Phosgene	CH <sub>2</sub> Cl <sub>2</sub>	Turn on	4nM	The test paper	[11]
	Phosgene	CH <sub>3</sub> CN	Turn on	0.48 nM	The TLC plate	[12]
	Phosgene	CH <sub>3</sub> CN	Ratiometric	0.09nM	PCL nanofibre	[13]

	Phosgene	CH <sub>3</sub> CN	Turn on	6.3 nM	Test strip	[14]
	Phosgene	CH <sub>3</sub> CN	Turn off	21.53 μM	Detection of phosgene in household bleach, Dipstick method, soil analysis	<b>This work</b>

## 10. References:

1. M. Shortreed, R. Kopelman, M. Kuhn, B. Hoyland, *Anal. Chem.*, 1996, **68**, 1414. (b) W. Lin.; Yuan, L.; Cao, Z.; Feng, Y.; Long, L. *Chem. Eur. J.* 2009, **15**, 5096. (c) Zhu, M.; Yuan, M.; Liu, X.; Xu, J.; Lv, J.; Huang, C.; Liu, H.; Li, Y.; Wang, S.; Zhu, D. *Org. Lett.* 2008, **10**, 1481-1484.
2. R. G. Parr, *Annu. Rev. Phys. Chem.*, 1983, **34**, 631–656.
3. (a) V. Barone and M. Cossi, *J. Phys. Chem. A*, 1998, **102**, 1995; (b) M. Cossi and V. Barone, *J. Chem. Phys.*, 2001, **115**, 4708; (c) M. Cossi, N. Rega, G. Scalmani and V. Barone, *J. Comp. Chem.*, 2003, **24**, 669.
4. A. D. Becke, *J. Chem. Phys.*, 1993, **98**, 5648.
5. C. Lee, W. Yang and R. G. Parr, *Phys. Rev. B*, 1998, **37**, 785.
6. M. E. Casida, C. Jamoroski, K. C. Casida and D. R. Salahub, *J. Chem. Phys.*, 1998, **108**, 4439; R. E. Stratmann, G. E. Scuseria, M. J. Frisch, *J. Chem. Phys.*, 1998, **109**, 8218; R. Bauernschmitt and R. Ahlrichs, *Chem. Phys. Lett.*, 1996, **256**, 454.
7. N. Sieffert and G. Wipff, *Dalton Trans.*, 2015, **44**, 2623–2638.
8. S. Saha and P. Sahoo, *Environ. Sci. Process. Impacts*, 2023, **25**, 1144–1149.
9. L. Bai, W. Feng and G. Feng, *Dyes Pigm.*, 2019, **163**, 483–488.
10. R. Abhijnakrishna and S. Velmathi, *Analyst*, 2023, **148**, 2267–2276.
11. J. Zhu, X. Mu, S. Zhang, L. Yan and X. Wu, *Spectrochim. Acta A Mol. Biomol. Spectrosc.*, 2021, **251**, 119485.
12. L. Bai, W. Feng and G. Feng, *Dyes Pigm.*, 2019, **163**, 483–488.
13. K. Maiti, D. Ghosh, R. Maiti, V. Vyas, P. Datta, D. Mandal and D. K. Maiti, *J. Mater. Chem. A Mater. Energy Sustain.*, 2019, **7**, 1756–1767.
14. L. Huang, W. Ye, Y.-T. Su, Z.-Y. Wu and H. Zheng, *Dyes Pigm.*, 2020, **173**, 107854.